IDŐJÁRÁS

Quarterly Journal of the Hungarian Meteorological Service
Vol. 108, No. 3, July–September 2004, pp. 173–194

Connections between urban heat island and surface parameters: measurements and modeling

János Unger[1], Zsolt Bottyán[2], Zoltán Sümeghy[1] and Ágnes Gulyás[1]

[1]*Department of Climatology and Landscape Ecology, University of Szeged, P.O. Box 653, H-6701 Szeged, Hungary*

E-mail: unger@geo.u-szeged.hu; sumeghy@geo.u-szeged.hu; agulyas@geo.u-szeged.hu

[2]*Department of Resource Economy, University of Debrecen, P.O. Box 10, H-4015 Debrecen, Hungary, E-mail: zbottyan@helios.date.hu*

(Manuscript received May 5, 2003; in final form September 26, 2003)

Abstract—This study deals with the influence of urban surface factors on the air temperature patterns, using mobile measurements under different weather conditions in the periods of March 1999 – February 2000 and April – October 2002. The studied city (Szeged, Hungary) is located on a plain with a population of 160,000. Investigations concentrated on the urban heat island (UHI) at its strongest development during the diurnal cycle. Tasks included: (1) Determination of spatial distribution of UHI intensity and some urban surface parameters (built-up and water surface ratios, sky view factor, building height). (2) Development of statistical models in the heating and non-heating seasons using the above mentioned parameters and their areal extensions. (3) Identification of similarities or differences in the seasonal spatial patterns of UHI along an urban cross-section and explanation these features using land-use and climatological parameters.

In both seasons the spatial distribution of UHI intensity fields has a concentric shape with some local irregularities. The intensity reaches more than 2°C (heating season) and 3°C (non-heating season) in the centre. According to the model equations determined by stepwise multiple linear regression analysis, there are clear connections between the spatial distribution of the urban excess temperature and the examined land-use parameters. Among these parameters sky view factor and building height are the most determining factors, which are in line with the urban surface energy balance. Along the cross-section the UHI intensity has a seasonal change, as a consequence of the prevailing weather conditions. The role of cloudiness and wind speed is clearly recognized during most of the time in the studied period. Utilization of normalized values shows that the form of the seasonal UHI profile is independent of the seasonal climatological conditions, and is determined by urban surface factors to a high degree.

Key-words: urban heat island, spatial and seasonal patterns, statistical model equations, urban cross-section, seasonal profiles.

1. Introduction

Urbanization modify materials, structure, and energy balance of the surface and air composition compared to the natural surroundings. As a consequence of the effects of these artificial factors, a distinguished local climate (urban climate) develops in the cities, which manifests itself by the excess temperature (urban heat island – UHI) most obviously. The magnitude of this excess is the UHI intensity (namely ΔT, the temperature difference between urban and rural areas). Generally, in its diurnal cycle the strongest development occurs 3–5 hours after sunset.

Simulation of real factors and physical processes generating the urban climate is difficult because of the complicated urban terrain with regard to surface geometry and materials, as well as artificial production of heat and air pollution. The detection of these factors and processes demands complex and expensive instruments, and sophisticated numerical and physical models. Despite these difficulties, several models have been developed for small-scale climate variations within the city. Some of these models are based on advective (*Oke*, 1976), energy balance (*Tapper et al.*, 1981; *Johnson et al.*, 1991; *Myrup et al.*, 1993; *Ruffieux*, 1995), radiation (*Voogt* and *Oke*, 1991), heat storage (*Grimmond et al.*, 1991), water balance (*Grimmond* and *Oke*, 1991), and surface sensible heat flux (*Voogt* and *Grimmond*, 2000) approaches. In order to study microclimate alterations within the city, utilization of statistical modeling may provide useful quantitative information about the urban temperature excess by employing different surface parameters (e.g. *Outcalt,* 1972; *Oke*, 1981, 1988; *Park*, 1986, 1987; *Kuttler et al.*, 1996; *Matzarakis et al.*, 1998).

Our objective is to investigate the seasonal effects and interactions inside the city on the air temperature, a few hours after sunset, when the UHI effect is generally most pronounced. To achieve this aim, we construct horizontal isotherm maps to show the average spatial distribution of the UHI intensity in the investigated periods and present some obvious relationships between temperature patterns and urban factors. Then we examine the quantitative effects of the relevant surface factors and their combinations on the patterns of the urban-rural temperature differences. The selection of these parameters, namely built-up ratio, water surface ratio, sky view factor, and building height, is based on their role in small-scale climate variations (*Oke*, 1987; *Golany*, 1996). Finally, we identify similarities or differences in the spatial distributions of ΔT by seasons along an urban cross-section and explain these features using land-use and climatological parameters.

2. Environmental conditions

The studied city, Szeged, is located in the south-eastern part of Hungary (46°N, 20°E) at 79 m above sea level on a flat flood plain. River Tisza passes through the city, otherwise, there are no large water bodies nearby. The river is relatively narrow and, according to our earlier investigation, its influence is negligible (*Unger et al.* 2000, 2001). These environmental conditions make Szeged a suitable place for studying an almost undisturbed urban climate.

Most of Hungary belongs to Köppen's climatic region Cf (temperate warm climate with a fairly uniform annual distribution of precipitation). Climatic subregions are distinguished using the mean temperature of vegetative season (t_{VS} in °C) and the aridity index ($H = Q^*/L_V P$ where Q^* is the annual mean net radiation in MJ m^{-2}, L_V is the latent heat of evaporation in MJ kg^{-1} and P is the annual mean precipitation in kg m^{-2}). The climate is arid or humid, according to whether the dimensionless H is bigger or less than 1, respectively. Szeged is in the *warm-dry* subregion by this classification, which is characterized by $t_{VS} > 17.5$°C and $H > 1.15$ (*Unger*, 1999). Two half years can be distinguished from the point of view of city dwellers: the heating (from October until April) and the non-heating (from April until October) seasons.

Szeged has an administration district of 281 km^2 with a population of 160,000. The base of the street network is a circuit-avenue system. Different land-use types are present including a densely-built centre with medium-wide streets and large housing estates of high concrete buildings set in wide green spaces. There are zones used for industry and warehousing, areas occupied by detached houses, considerable open spaces along the riverbanks, in parks, and around the city's outskirts (*Unger et al.*, 2000).

3. Parameters and methods

3.1 Grid network

Our efforts were focused on the urbanized part of the administration district. The area of investigation was divided into two sectors and subdivided further into 0.5 km × 0.5 km square cells (*Fig. 1*). The same grid size was employed, for example, in an investigation of UHI in Seoul, Korea (*Park*, 1986). The original study area consists of 107 cells covering the urban and suburban parts of Szeged, mainly inside of the circle dike that protects the city from river floods. The outlying parts, characterized by mostly rural features, are not included in the network except for four cells on the western side of the area, which are necessary to determine the temperature contrast between urban and

rural areas. The grid was established by quartering the 1 km × 1 km square network of 1:10,000 scale maps of the Unified National Mapping System developed for the topographical maps of Hungary (*Unger et al.*, 2000, 2001).

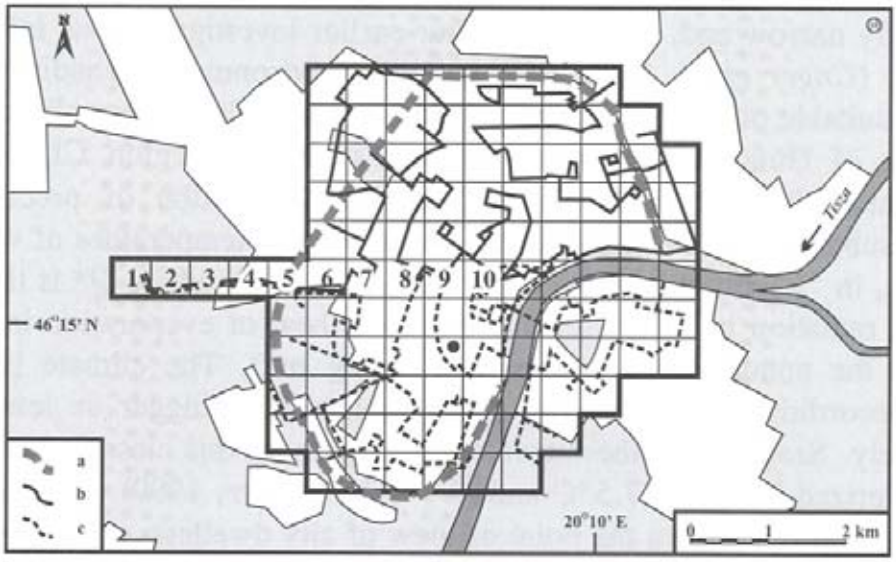

Fig. 1. Division of the area of study into 0.5 km × 0.5 km grid cells. The dashed line (*a*) denotes the circle dike, (*b*) and (*c*) are the measurement routes in the northern and southern sectors, respectively. The permanent measurement site of the University of Szeged is indicated as •, and the cells of cross-section are numbered from 1 to 10.

In the present research, six southern and four western cells of the original study area are omitted because of the lack of one parameter in the data set (building height, see Section 3.5). Therefore, we employ altogether 97 cells covering an area of 24.25 km^2.

3.2 Temperature (maximum UHI intensity)

In order to collect data on ΔT for every cell, mobile measurements were performed on fixed return routes once a week during the period of March 1999–February 2000 (*Fig. 1*). In case of surface and near-surface air UHI measurements, vehicle-based observation (car, tram, helicopter, airplane, satellite) is a common process (e.g., *Conrads* and *van der Hage*, 1971; *Oke* and *Fuggle*, 1972; *Johnson*, 1985; *Moreno-Garcia*, 1994; *Yamashita*, 1996; *Voogt* and *Oke*, 1997; *Klysik* and *Fortuniak*, 1999). Altogether 48 car traverses were taken, 24 in the northern, and another 24 in the southern sector. The frequency of traverses provided sufficient information under different weather conditions, except for rain.

Division of the area of the study into two sectors was necessary because of the large number of cells. The 75 km and 68 km long return routes in the northern and southern sectors, respectively, were needed to make time-based corrections, since measurements took about 3 hours. Temperature readings were obtained using a radiation-shielded resistance sensor connected to a data logger for digital sampling. Data were collected every 16 sec, so at an average car speed of 20–30 km h^{-1}, the average distance between measuring points was 89–133 m. In order to avoid the influence of engine and exhaust heat, the sensor was mounted 0.60 m in front of the car at 1.45 m above the ground. The speed was sufficient to provide adequate ventilation for the sensor to measure the ambient air temperature. The traffic density in the late hours of measurements was rather low. The logged values at forced stops (e.g., at traffic lamps) were rejected from the data set.

Having averaged the measurement values by cells, time adjustments to a reference time were applied assuming linear air temperature change with time. This change was monitored by the continuous records of the automatic weather station of the University of Szeged (*Fig. 1*). The linear adjustment appears to be correct for data collected a few hours after sunset in urban areas. However, because of the different time variations of cooling rates, it is only approximately correct for suburban and rural areas (*Oke* and *Maxwell*, 1975). The reference time, namely the likely time of the occurrence of the strongest UHI in the diurnal course, was 4 hours after sunset, a value based on earlier measurements. Consequently, we can assign one temperature value to every cell in the northern sector or in the southern sector at a given measuring night. These values refer to the centre of each cell.

UHI intensities were determined by cells referring to the temperature of the westernmost cell (1) of the original area of the study ($T_{cell} - T_{(1)}$), which was regarded as a rural cell because of its location outside of the city (*Fig. 1*). Moreover, the weather station of the Hungarian Meteorological Service is located there, and its records were used as rural (reference) data in the earlier studies on the urban climate of Szeged (e.g., *Unger*, 1996, 1999).

The 97 points (the above mentioned cell centerpoints) covering the urban parts of Szeged provide an appropriate basis to interpolate isolines (temperature and other parameters) using a geostatistical gridding method, the standard Kriging procedure.

3.3 Built-up and water surface ratio

Ratios of the built-up (covered surface – building, street, pavement, parking lot, etc.) (*B*) and water surface (*W*) by cells were determined by a vector and raster-based GIS database combined with remote sensing analysis of SPOT XS

images. The digital satellite image was rectified to the Unified National Mapping System using 1:10,000 scale maps. The nearest-neighbour method of resampling was employed, resulting in a root mean square value of less than 1 pixel. The geometric resolution of the image was 20 m × 20 m.

Normalized Difference Vegetation Index was calculated from the pixel values, using visible (0.58–0.68 μm) and near infrared (0.72–1.1 μm) bands (*Gallo* and *Owen*, 1999). They are between −1 to +1 indicating the effect of green space in the given spatial unit. Using these values, built-up, water, and vegetated surfaces were distinguished and their ratios (to total cell area) for each grid square were determined using cross-tabulation (*Unger et al.*, 2000). In the Szeged region the occurrence of non-vegetated (bare) areas is negligible, namely, each non-built-up place is covered by some vegetation (e.g., garden and cultivated plants, trees, grass, bushes, weeds).

3.4 Sky view factor

The built-up ratio does not describe completely the characteristics of an artificial urban surface. Streets and buildings create canyons, and this 3D geometry plays an important role in the development of UHI. Namely, heat transport and outgoing long wave radiation decrease because of the moderated turbulence and increased obstruction of the sky.

To estimate the openness of the cell surfaces quantitatively, we applied the sky view factor (*SVF*, now marked shortly by *S*). It is a dimensionless measure (between 0 and 1) of the degree to which sky is obscured by the surroundings for a given point (*Oke*, 1981, 1988). Commonly, *S* is determined using either analytical or photographic methods, employing theodolite, fish-eye lens (digital) camera, or automatic canopy analyzer (*Oke*, 1981; *Bärring et al.*, 1985; *Park*, 1987; *Grimmond et al.*, 2001).

In our analytical method we have measured two elevation angles to the top of the buildings (α_1 and α_2) perpendicularly to the axis of streets in both directions, using an 1.5 m high theodolite. From these data, wall view factors can be calculated to the left (WVF_{W1}) and right (WVF_{W2}) sides (*Oke*, 1981). The measuring points are not always coincident with the midpoint of the distance between buildings on both sides (*Fig. 2*). The calculation of *S* is based on *Oke's* (1988) results (for explanation of symbols see *Fig. 2*):

$$WVF_{W1} = (1 - \cos\alpha_1)/2 \qquad \text{where } \alpha_1 = \tan^{-1}(H_1/W_1), \tag{1}$$

$$WVF_{W2} = (1 - \cos\alpha_2)/2 \qquad \text{where } \alpha_2 = \tan^{-1}(H_2/W_2), \tag{2}$$

$$S = 1 - (WVF_{W1} + WVF_{W2}). \tag{3}$$

In order to determine S values, the same long canyons (measuring routes) were used as for temperature sampling. 532 points were surveyed by theodolite, and the values of S were also averaged by cells. In line with the temperature sampling, the distance between the points was 125 m on average. Angle measurements taken higher within a canyon (1.5 m) excluded more of the terrain (non-sky) and resulted in an over-estimate of S after the calculation. This effect is more pronounced in canyons with low H/W ratios (*Grimmond et al.*, 2001). Due to technical difficulties, we did not have any measurement points at the intersections of roads, so the calculated S values are probably a bit smaller than the real ones. Furthermore, if there were parks, forests, or water surface in a particular direction, we assigned 0° as an angle value, because it is difficult to determine S values modified by the vegetation, and the results are not unambiguous (*Yamashita et al.*, 1986).

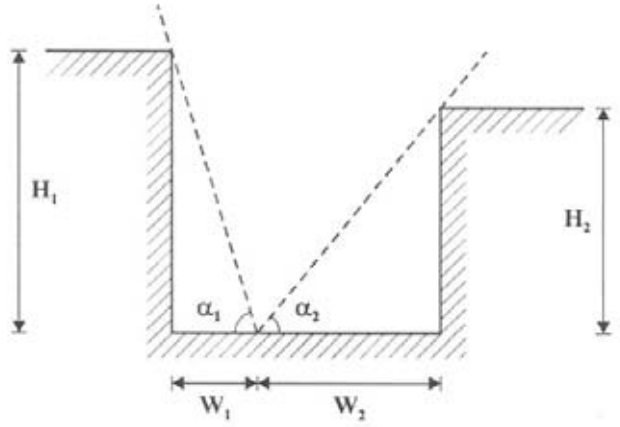

Fig. 2. Geometry of a non-symmetric canyon flanked by buildings with a measuring point not at the centre of the floor (modified after *Oke*, 1988).

While earlier investigations were limited to the centre or only some parts of the cities and used far smaller numbers of measurements (*Oke*, 1981, 1988; *Johnson*, 1985; *Yamashita et al.*, 1986; *Park*, 1987; *Eliasson*, 1996; *Grimmond et al.*, 2001), the obtained data set represents almost the total urban area.

3.5 Building height

Since some areas with different land-use features can produce almost equal S data (narrow street with low buildings versus broad street with high buildings), S values alone do not describe sufficiently the vertical geometry of cities. It is important to have quantitative information on the vertical size of a canyon, because it plays significant role in the energy budget.

To determine the vertical dimension of a canyon, we applied a combined procedure. The above mentioned elevation angles (α_1 and α_2) are available at each point. If we have the distances to the walls from the measuring point (W_1 and W_2, see *Fig. 2*), there is a simple formula to calculate wall heights (H_1 and H_2), taking the instrument height of 1.5 m into account:

$$H_1 = \tan \alpha_1 \, W_1 + 1.5 \text{ m}, \tag{4}$$

$$H_2 = \tan \alpha_2 \, W_2 + 1.5 \text{ m}. \tag{5}$$

The width of the streets was determined by means of aerial photographs concerning any part of the street. After digitizing these images, we made an orthophoto of Szeged using the Ortho Base tool of the ERDAS IMAGINE GIS software, and marked the measurement points. This orthophoto is already suitable to determine distances of the walls (W_1 and W_2) from the measurement points. As the aerial photographs do not cover completely the area of the study, these distances are not available for six and four cells in the southern and western parts of Szeged, respectively.

3.6 The applied statistical model

In order to assess the extent of the relationships between the mean maximum UHI intensity (ΔT) and various urban surface factors, multiple correlation and regression analyses were applied. Some examples of the modeled variables and employed variable parameters of earlier studies are in *Table 1*.

In the course of determination of model equations we used ΔT as predictant (dependent variable) in both seasons and the afore-mentioned parameters as predictors: ratios of built-up surface (B) and water surface (W) as a percentage, mean sky view factor (S), mean building height (H) in m by cells. Searching for statistical relationships, we have to take into account that our parameters are variables (spatially) and constants (temporally) at the same time. Since these parameters change rapidly with the increasing distance from the city center, we applied the exponentially distance-weighted spatial means of the mentioned land-use parameters for our model. The distance scale of the weight should be derived from the transport scale of the heat in the urban canopy. Our statistical model determined this scale from the measured parameter values. A set of predictors concerning all four basic urban parameters were originated as areal extensions and grouped in the following way:

Group 1: parameter values (S, H, B, W) in the cell with $\Delta i^2 + \Delta j^2 = 0$.

Group 2: mean parameter values ($S1$, $H1$, $B1$, $W1$) of all cells with $0 < \Delta i^2 + \Delta j^2 < 2^2$.

Group 3: mean parameter values ($S2$, $H2$, $B2$, $W2$) of all cells with $2^2 < \Delta i^2 + \Delta j^2 < 4^2$.

Here i and j are cell indices in the two dimensions, while Δi and Δj are the differences of cell indices with respect to a given cell. These zones cover the entire investigated model area of Szeged.

Table 1. Survey of some studies using statistical models for prediction of UHI (extended after *Unger et al.*, 2000)

Predicted variable	Employed parameters	Reference
UHI intensity	Wind speed, cloudiness	*Sundborg* (1950)
UHI intensity	Population, wind speed	*Oke* (1973)
Max. UHI intensity	Population	
UHI intensity	Wind speed, cloudiness, atmospheric stability, traffic flow, energy consumption, temperature	*Nkemdirim* (1978)
UHI intensity at four different air levels	Lapse rate, wind speed, ratio of lapse rate to wind speed	*Nkemdirim* (1980)
UHI intensity	Wind speed, land-use type ratios	*Park* (1986)
Max. UHI intensity	Impermeable surface, population	
UHI intensity	Wind speed, cloudiness, temperature, humidity mixing ratio	*Goldreich* (1992)
UHI intensity	Wind speed, cloudiness, air pressure	*Moreno-Garcia* (1994)
Surface UHI intensity	Solar radiation, wind speed, cloudiness	*Chow et al.* (1994)
UHI intensity	Built-up area, height, wind speed, time, temperature amplitude	*Kuttler et al.* (1996)
UHI intensity for T_{avg}, T_{max}, T_{min}	NDVI, surface temperature (satellite-based)	*Gallo* and *Owen* (1999)
UHI intensity	Distance from the city centre, built-up ratio	*Unger et al.* (2000)
UHI intensity	Wind speed, cloudiness	*Morris et al.* (2001)

With these areal extensions we have 12 predictors to construct the linear statistical model. However, there could be some multi-colinearity among these parameters. In order to eliminate these multi-colinearities, the set of parameters have to be selected. Using the cross-correlation matrix of these predictors we can find the highest correlation coefficients, which means strong connections among them. To avoid the unreasonable reduction of the number of predictors, only the parameter with maximum absolute mean of its correlation coefficients was taken out of each group.

The method for the construction of model equations is the stepwise multiple linear regression. The applied implementation of this procedure is part of the SPSS 9 statistical software. A comprehensive discussion of the mathematical background of this method is found in *Miller* (2002). Predictors were entered or removed from the model depending on the significance of the F value of 0.01 and 0.05, respectively. Since there is a well noticeable difference between the magnitudes of ΔT fields in these seasons, under these conditions two linear statistical model equations were determined: one for the heating and one for the non-heating season.

3.7 Cross-section investigation

A small but representative part of the original area of the study (altogether 10 cells) is examined seasonally in detail. This is an overlapping part between the northern and southern sectors (*Fig. 1*), namely a cross-section in the urban area, which consists of cells stretching from the rural area (cell 1) to the city core (cell 10) with a distance of 4.5 km.

The profiles of the UHI intensity along the cross-section were investigated by comparison of absolute and normalized seasonal means taking land-use and climatological features into consideration. The normalized values by cells are the ratios of the absolute means of a given cell and cell 10 (where ΔT is the highest in all seasons). Since meteorological conditions (first of all wind speed and cloudiness) influence the absolute values (in °C) of the UHI intensity (e.g., *Landsberg*, 1981; *Park*, 1986; *Yagüe et al.*, 1991; *Unger*, 1996), the seasonal comparison of spatial variation of ΔT is more effective using normalized values. Namely, the profile of the normalized seasonal mean UHI intensity is expected to be independent of the prevailing weather conditions in the studied period; nevertheless, it is expected to be dependent on the surface factors (e.g., land-use features, distance from the city centre, etc.).

4. Results and discussion

4.1 Spatial characteristics of the urban parameters and UHI

The spatial distribution of the built-up ratio in the city has almost a concentric shape decreasing from the central areas to outwards (*Fig. 3a*). The densely built-up areas are concentrated in the middle and north-eastern parts of the city with maximum values more than 96%. River Tisza with its environment has a low built-up ratio and, of course, a high water surface ratio which can be clearly recognized with its east-to-south curve (*Fig. 3b*). Apart from this, the

extension of water surfaces is negligible, except for some small and shallow recreational lakes in the western part of the city.

Due to the significant variability of the building height and width of the streets, the sky view factor pattern is very complicated (*Fig. 3c*). This field does not form a circular structure and its extreme values are not located only in the centre. There are three parts of the city where S is low (with values of lower than 0.8), and in the centre it is lower than 0.7. The highest buildings are concentrated in the north-eastern part of the city with maximum values of about 20 m (*Fig. 3d*). There is an other area in the southern central region, where the buildings are higher than 15 m. Generally, the average building height is more than 10 m in the studied area.

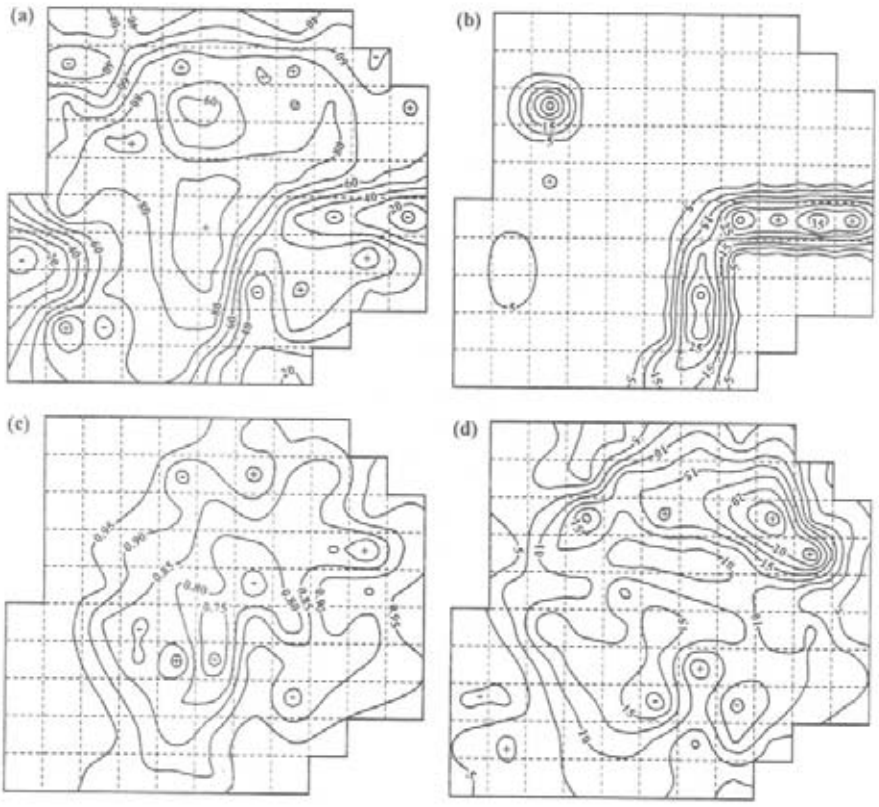

Fig. 3. Spatial distribution of (*a*) the ratio of the built-up area, (*b*) the ratio of the water surface to the total area (in percent), (*c*) the average sky view factor values and (*d*) the average building heights (in m) by cells in Szeged.

In the non-heating season (*Fig. 4a*), the greatest mean UHI intensity (3.18 C) is found in the central cell, and the ΔT of higher than 2 C – indicating significant thermal modification caused by urbanization – covers about 37% of the investigated area. In the heating season (*Fig. 4b*), the highest value of the

UHI intensity (2.12°C) occurs in the central cell, too, but the area of considerable differences (>2°C) covers only about 2% of the total area (*Unger et al.*, 2000).

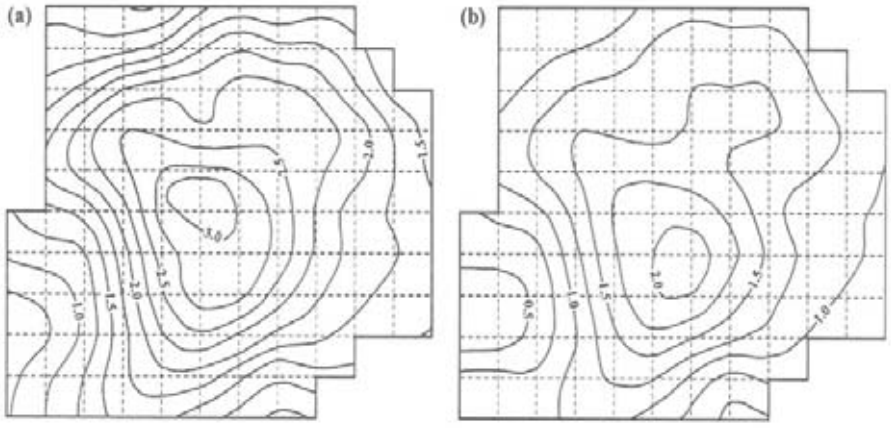

Fig. 4. Spatial distribution of the measured mean maximum UHI intensity (°C) during (*a*) the non-heating season (April 16 – October 15: 26 measurements) and (*b*) the heating season (October 16 – April 15: 22 measurements) in Szeged.

The most obvious common features of the UHI patterns are that the isotherms show almost concentric shapes in both seasons (*Fig. 4*). A deviation from this shape occurs in the north-eastern part of the city, where the isotherms stretch towards the suburbs. This anomaly can be explained by the effect of the large housing estates with high concrete buildings located mainly in the north-eastern part of the city with a built-up ratio higher than 75% (*Fig. 3a*), a sky view factor less than 0.85 (*Fig. 3c*), and a building height more than 15 m (*Fig. 3d*). The second irregularity is caused by the cooling influence of River Tisza, because along the river the isotherms are a bit drawn back towards the centre. The third area of anomaly can be found in the western part of the city, where the surface geometry changes abruptly along a westbound transect (which starts at the centre). This region is characterized by S values higher than 0.95, building heights lower than 7 m, and built-up ratio of about 25%.

The seasonal differences in the spatial distribution of ΔT (in °C) may be formed rather as a consequence of different weather characteristics of the two seasons than as a consequence of heating or non-heating of dwellings. In the Szeged region the climate conditions in winter, conducing to the formation of UHI, are less common (*Table 2*). Thus, in the warmer (non-heating) season, the role of the weather conditions (stronger solar radiation, more frequent clear sky, and weak wind) and the reduced latent heat transport, due to the more impermeable and guttered urban terrain, is more pronounced in the

development of UHI than the anthropogenic heat emission by heating in the colder season (*Unger et al.*, 2000).

Table 2. Monthly and seasonal means of the selected meteorological parameters in Szeged (March 1999 – February 2000)

Period	M	A	M	J	J	A	S	O	N	D	J	F	Spr.	Sum.	Aut.	Win.
Wind speed ($m\ s^{-1}$)	3.5	3.5	2.6	2.5	2.6	2.1	2.7	2.9	2.6	3.4	3.5	3.4	3.2	2.4	2.7	3.4
Cloudiness (okta)	4.7	4.9	4.3	4.6	3.8	3.6	3.6	4.5	5.9	5.6	6.1	3.7	4.6	4.0	4.7	5.1

4.2 Statistical model equations

Table 3 contains the cross-correlation matrix of the predictors and maximum absolute means of the correlation coefficients by lines. As a result of the selection procedure to reduce the multi-colinearities, three parameters (*S*, *H*1, and *S*2) were taken out of the original parameter-set. Thus, for the construction of the model equations, nine predictors remained.

Table 3. Cross-correlation matrix of the parameters and absolute means of the correlation coefficients by lines. Parameters are taken out of the models, and their absolute means are marked with bold setting (see Section 3.3–3.6 for explanation)

Parameter	B	S	W	H	B1	S1	W1	H1	B2	S2	H2	W2	Abs. mean
B	-	-0.50	-0.48	0.52	0.62	-0.50	-0.24	0.45	0.11	-0.12	0.01	-0.12	0.33
S	-0.50	-	0.13	-0.72	-0.52	0.64	0.09	-0.55	-0.05	0.41	-0.33	0.02	**0.36**
W	-0.48	0.13	-	-0.16	-0.13	0.02	0.29	-0.10	0.04	-0.22	0.18	0.16	0.17
H	0.52	-0.72	-0.16	-	0.43	-0.50	-0.16	0.57	-0.01	-0.42	0.23	-0.11	0.34
B1	0.62	-0.52	-0.13	0.43	-	-0.64	-0.49	0.57	0.15	-0.14	0.06	-0.21	0.36
S1	-0.50	0.64	0.02	-0.50	-0.64	-	0.04	-0.84	-0.04	0.56	-0.49	0.08	0.39
W1	-0.24	0.09	0.29	-0.16	-0.49	-0.04	-	-0.14	-0.08	-0.27	0.17	0.24	0.20
H1	0.45	-0.55	-0.10	0.57	0.57	-0.84	-0.14	-	-0.03	-0.63	0.48	-0.08	**0.40**
B2	0.11	-0.05	0.04	-0.01	0.15	-0.04	-0.08	-0.03	-	-0.10	0.21	0.02	0.08
S2	-0.12	0.41	-0.22	-0.42	-0.14	0.56	-0.27	-0.63	-0.10	-	-0.85	-0.10	**0.35**
H2	0.01	-0.33	0.18	0.23	0.06	-0.49	0.17	0.48	0.21	-0.85	-	0.13	0.28
W2	-0.12	0.02	0.16	0.23	-0.21	0.08	0.24	-0.08	0.02	-0.10	0.13	-	0.12

In both seasons the order of significance of the applied parameters is the same, but in the heating season the role of them is more pronounced than in the non-heating season. The model equations have four predictors, among them the $S1$ predictor is the most important, but H and $B1$ factors also play important role in both seasons (*Table 4*).

Table 4. Values of the stepwise correlation of mean maximum UHI intensity (ΔT) and urban surface parameters, and their significance levels in the studied periods in Szeged (n = 97) (see Section 3.3–3.6 for explanation)

Period	Parameter entered	Multiple |r|	Multiple r^2	Δr^2	Significance level (%)
April 16 – October 15 (non-heating season)	S1	0.806	0.649	0.000	0.1
	S1, H	0.845	0.714	0.065	0.1
	S1, H, B1	0.863	0.744	0.030	0.1
	S1, H, B1, W1	0.902	0.814	0.070	0.1
October 16 – April 15 (heating season)	S1	0.791	0.626	0.000	0.1
	S1, H	0.834	0.696	0.070	0.1
	S1, H, B1	0.852	0.726	0.030	0.1
	S1, H, B1, W1	0.873	0.762	0.036	0.1

The four-variable models for the non-heating (nh) and heating (h) seasons indicate strong linear relation between the mean maximum UHI intensity and the applied land-use parameters (*Table 4*). The model equations for ΔT_{nh} and ΔT_h (in °C) are the next (*Table 5*):

$$\Delta T_{nh} = -4.291S1 + 0.035H + 0.023B1 + 0.042W1 + 3.824, \quad (6)$$

$$\Delta T_h = -3.242S1 + 0.025H + 0.014B1 + 0.021W1 + 3.036. \quad (7)$$

The absolute values of the multiple correlation coefficients (r) between ΔT and the studied parameters are 0.902 and 0.873 in the non-heating and heating seasons; both are significant at 0.1% level. This means that with these four parameters we are able to explain 81.4% and 76.2% of the above mentioned relationships in the studied periods *(Table 4)*. The standard errors of the estimates are 0.272 and 0.218 in the non-heating and heating half year, respectively.

We used these two model equations ((6) and (7)) to determine the spatial distribution of ΔT patterns in the studied area (*Fig. 5*). There is a considerable similarity between the measured and predicted UHI intensity fields in both seasons, namely, they have the same irregularities, however, some differences can be detected (*Fig. 4* and *Fig. 5*).

Table 5. Values of significance, coefficients, and standard errors of the applied urban surface parameters of the models in the studied periods in Szeged (n = 97) (see Section 3.3–3.6 for explanation)

Period	Parameter	Significance	Coefficient	Standard error
April 16 – October 15 (non-heating season)	S1	0.000	**-4.291**	0.787
	H	0.000	**0.035**	0.006
	B1	0.000	**0.023**	0.003
	W1	0.000	**0.042**	0.007
	Const.	0.000	**3.824**	0.897
October 16 – April 15 (heating season)	S1	0.000	**-3.242**	0.631
	H	0.017	**-0.025**	0.005
	B1	0.006	**0.014**	0.003
	W1	0.022	**0.021**	0.006
	Const.	0.000	**3.036**	0.718

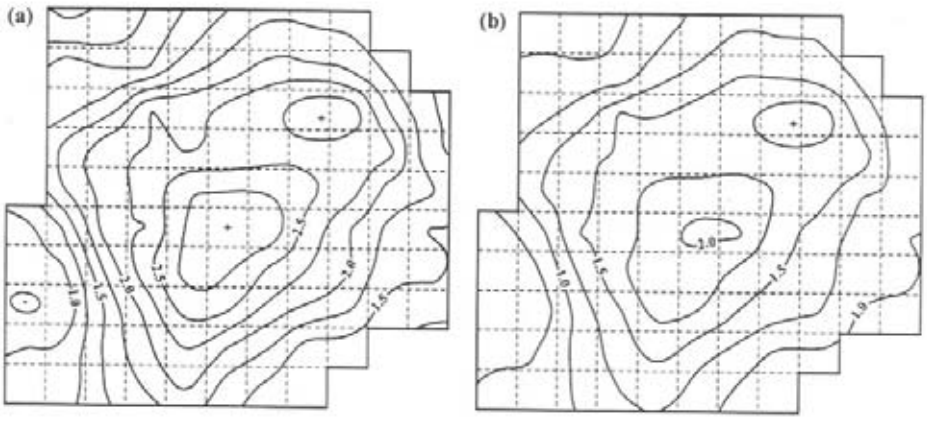

Fig. 5. Spatial distribution of the predicted mean max. UHI intensity (°C) during the (*a*) non-heating season and (*b*) the heating season in Szeged.

We compared the results of the model to an independent UHI intensity data set measured during the non-heating half year in 2002. The studied area and the mobile sampling method were the same as in the earlier cases, except that we used two cars to take temperature measurements at the same time in the two sectors, altogether 18 times. According to *Fig. 6a*, the measured independent UHI intensity pattern is similar to the one mentioned above (*Fig. 5a*), though the largest ΔT value is smaller by about 0.5°C. After that we calculated the spatial distribution of the difference between the predicted and measured independent UHI intensities (*Fig. 6b*). We can find only two small areas where the absolute UHI intensity anomaly is between 0.4°C and 0.6°C.

In the north-eastern part of the city, the predicted values are lower than the measured ones (negative anomaly). At the western border of the investigated area the predicted values are higher than the measured ones (positive anomaly). However, these areas occupy only a minor part of the area of the study (about 3.9 cells, 1 km^2, 4% of the total area). The areas characterized by the differences lower than 0.2°C are significantly larger, covering altogether 73 cells (about 18,2 km^2, 75%).

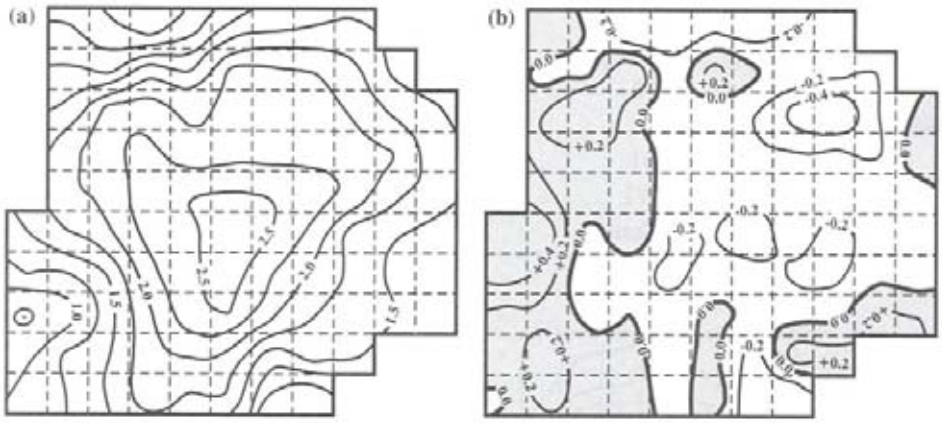

Fig. 6. (*a*) Spatial distribution of the measured mean max. UHI intensity (°C) during the independent non-heating season in 2002 and (*b*) spatial distribution of the difference of measured and predicted mean max. UHI intensity (°C) during the same season in Szeged.

It can be established that our model described the spatial distribution of the real UHI intensity field in the investigated area rather correctly. On the basis of our results, we may apply this model-construction procedure to predict the ΔT for other cities of different size and even non-concentric shape.

4.3 Cross-section profiles of UHI by seasons

Table 6 contains the areal ratios (%) of the main land-use types by cells along the selected cross-section. The largest built-up density (more than 90%) can be found around the centre (see cells 9 and 10 in *Fig. 1*), but the variation from the urban edge to the core is not uniform. The proportion of the water surface is rather negligible.

According to *Fig. 7a,* the profiles in every season show a marked increase from a rural level after reaching the edge of built-up areas (cell 3, see *Table 6*), and the highest values are in the city centre (cell 10). The absolute values of the seasonal profiles are almost the same in every cell, with the exception of winter. The values of the winter profile (with the largest seasonal

mean UHI intensity of 1.44°C) do not reach even the half of the values of other seasons. Because of the low winter values, the mean annual profile is a bit moderate compared to the ones of the first three seasons (the largest ΔT is 2.58°C).

Table 6. Land-use types by cells along the urban cross-section in Szeged

Land-use type (%)	Cell number									
	1	2	3	4	5	6	7	8	9	10
Built-up	0	0	18.9	70.4	54.2	85.6	71.7	77.8	91.4	90.5
Open	100	100	81.1	23.5	45.3	11.1	28.3	22.2	8.6	9.1
Water	0	0	0	6.1	0.5	3.3	0	0	0	0.4

Using normalized values, the differences among the seasonal profiles tend to disappear (*Fig. 7b*). These patterns follow remarkably well the general cross-section profile of the typical UHI described by *Oke* (1987): the 'cliff' is a steep temperature gradient at the rural/urban boundary, and much of the rest of the urban area appears as a 'plateau' of warm air with a steady but weaker horizontal gradient of increasing temperature towards the city centre. The urban core shows a final 'peak', where the largest temperature difference is observed (*Fig. 7c*).

In Szeged, the normalized ΔT values varied together along the cross-section with the largest deviation of only 0.13, in all seasons and in the whole one-year period (*Fig. 7b*). The 'cliff' with the large temperature gradient is located between cells 2 and 4 (the distance is 1 km). The profile shows a 1.5 km long thermal 'plateau' which is characterized by a very low temperature increment through its four cells (from 4 to 7). Then there is a second, very steep 'cliff' between the cells 7 and 8 (0.5 km), which indicates the onset of the 'peak' region. The areal extent of the largest values are rather wide (three cells, 1 km), so the steepness at the 'peak' value is relatively less sharp. This is explicable by the extent and homogeneity of the central urban part, which is dominated by 3–5 storey buildings built around the turn of the 19th and 20th centuries after the so called 'Great Flood' in 1879, which destroyed the city.

The seasonal variation of the urban temperature anomaly along the cross-section is attributed mainly to differences in weather conditions (*Table 2*). Winter months have the highest wind speed and cloudiness: at this time the UHI intensity is the weakest. In summer, when the above mentioned parameters have the smallest values, the extent of ΔT is not the largest in every point along the cross-section: it is slightly under or over the ΔT values in spring and autumn. These facts suggests that the effects of the climatological

parameters are fairly complex, and the investigation of their influence on the UHI cannot be restricted to only two, although important, parameters.

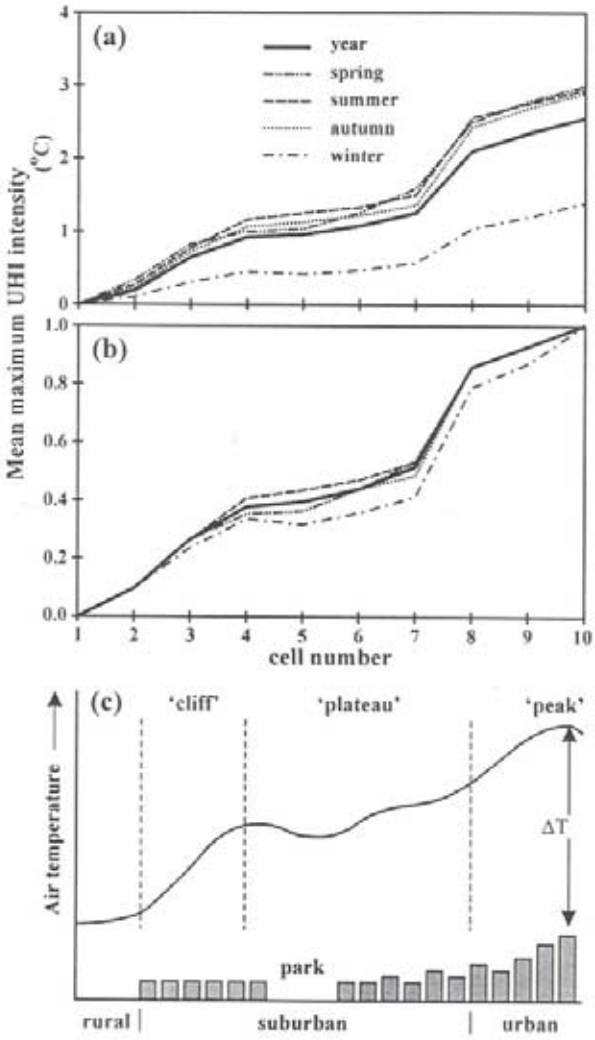

Fig. 7. Seasonal and annual profiles of (*a*) the absolute and (*b*) the normalized mean maximum UHI intensity across Szeged. (*c*) Generalized cross-section of the typical UHI after sunset (modified after *Oke*, 1987).

The use of the normalized values proved that the form of seasonal mean UHI profile depends only on surface factors. Among these factors, the built-up ratio may not be the most important one, because the steady, but not uniform increment of temperature towards the city core does not follow exactly the built-up density variation by cells (*Table 6*). However, an another parameter, however, the distance from the city centre seems to be more dominant in this general increasing tendency of urban temperature (*Unger et al.*, 2000).

5. Conclusions

In this paper the spatial and temporal features of the UHI effect was investigated in Szeged, Hungary. The following conclusions can be drawn from the analysis presented:

- The heat island phenomenon always appeared in the studied area, even though the UHI intensity changed during the year, as a consequence of the prevailing weather conditions, which vary by seasons in the temperate climatic region.
- The results on the seasonal spatial distribution of mean UHI indicate that:
  - (i) The spatial patterns of the UHI intensity have almost concentric shapes with the values decreasing from the central areas towards the outskirts. The anomalies are caused by the alterations in the urban surface factors.
  - (ii) There are significant differences in the magnitudes of the seasonal patterns. The area of the mean UHI intensity higher than 2°C is far larger in the non-heating than in the heating season.
- The statistical estimation of the spatial distribution of mean UHI intensity by the aid of surface parameters indicates that:
  - (i) On the basis of the statistical analysis there is a strong linear relationship between the mean UHI intensity and the studied urban parameters, such as sky view factor, building height, built-up ratio, water surface ratio, and their areal extensions in both seasons.
  - (ii) Generally, our model described the spatial distribution of the real UHI intensity field in the area of the study rather correctly, because the areas characterized by the differences lower than 0.2°C cover the larger parts of the city (75%). Nevertheless, there are small differences between the predicted and measured UHI fields, which are caused by some possible errors in the temperature samplings, the low number of studied parameters, and the considerable irregularities of the surface geometry.
  - (iii) This procedure, used to predict the UHI intensity, may be applicable for other cities of different size and even non-concentric shape, but for the true validation it is necessary to have complete databases of measured intensities for those cities.
- The profile of mean UHI and its seasonal variation along a cross-section indicates that:
  - (i) The seasonal profiles follow remarkably well the general cross-section of the typical UHI.

(ii) The role of cloudiness and wind speed on the seasonal variation of the UHI is clearly recognized throughout the one-year period.

(iii) The usefulness of the normalized values in the investigaton of the cross-section temperature distribution has been proved. It came to light, that the shape of the seasonal mean UHI profile is independent of the seasonal weather conditions, and it is determined mainly by the surface factors.

- Consequently, our preliminary results prove that the statistical approach on estimation of the UHI intensity in Szeged is promising. We are planning to extend this project by modeling urban thermal patterns as they are affected by weather conditions with a time lag. We intend to employ the same parameters used in this study, as well as additional urban and meteorological parameters, to predict the magnitude and spatial distribution of the UHI intensity on the days characterized by any kind of weather conditions (apart from precipitation), at any time of the year, without having recourse to extra mobile measurements. Although, adding meteorological predictors increase the complexity of the model, it may give us a useful tool for the prediction of the temperature field for several hours in advance.

Acknowledgements—The authors wish to give special thanks to *P. Purnhauser, E. Robotka,* and *Z. Zboray* who took part in the measurement campaigns and data pre-processing, and to the reviewers for their helpful suggestions. This research was supported by the grant of the Hungarian Scientific Research Fund (OTKA T/034161). The work of the first author was also supported by the Széchenyi István Grant of the Ministry of Education.

References

Bärring, L., Mattsson, J.O., and *Lindqvist, S.,* 1985: Canyon geometry, street temperatures and urban heat island in Malmö, Sweden. *Int. J. Climatol. 5,* 433-444.

Chow, S.D., Zheng, J., and *Wu, L.,* 1994: Solar radiation and surface temperature in Shangai City and their relation to urban heat island intensity. *Atmos. Environ. 28,* 2119-2127.

Conrads, L.A. and *van der Hage, J.C.H.,* 1971: A new method of air-temperature measurement in urban climatological studies. *Atmos. Environ. 5,* 629-635.

Eliasson, I., 1996: Urban nocturnal temperatures, street geometry and land use. *Atmos. Environ. 30,* 379-392.

Gallo, K.P. and *Owen, T.W.,* 1999: Satellite-based adjusments for the urban heat island temperature bias. *J. Appl. Meteorol. 38,* 806-813.

Golany, G.S., 1996: Urban design morphology and thermal performance. *Atmos. Environ. 30,* 455-465.

Goldreich, Y., 1992: Urban climate studies in Johannesburg, a sub-tropical city located on a ridge – A review. *Atmos. Environ. 26B,* 407-420.

Grimmond, C.S.B. and *Oke, T.R.,* 1991: An evapotranspiration-interception model for urban areas. *Water Resour. Res. 27,* 1739-1755.

Grimmond, C.S.B., Cleugh, H.A., and *Oke, T.R.,* 1991: An objective urban heat storage model and its comparison with other schemes. *Atmos. Environ. 25B,* 311-326.

Grimmond, C.S.B., Potter, S.K., Zutter, H.N., and *Souch, C.*, 2001: Rapid methods of estimate sky-view factors applied to urban areas. *Int. J. Climatol. 21*, 903-913.

Johnson, D.B., 1985: Urban modification of diurnal temperature cycles in Birmingham. *J. Climatol. 5*, 221-225.

Johnson, G.T., Oke, T.R., Lyons, T.J., Steyn, D.G., Watson, I.D., and *Voogt, J.A.*, 1991: Simulation of surface urban heat islands under 'ideal' conditions at night, I: Theory and tests against field data. *Bound.-Lay. Meteorol. 56*, 275-294.

Klysik, K. and *Fortuniak, K.*, 1999: Temporal and spatial characteristics of the urban heat island of Lódz, Poland. *Atmos. Environ. 33*, 3885-3895.

Kuttler, W., Barlag, A.-B., and *Roßmann, F.*, 1996: Study of the thermal structure of a town in a narrow valley. *Atmos. Environ. 30*, 365-378.

Landsberg, H.E., 1981: *The Urban Climate*. Academic Press, New York.

Matzarakis, A., Beckröge, W., and *Mayer, H.*, 1998: Future perspectives in applied urban climatology. *Proceed. The Second Japanese-German Meeting*. RCUSS, Kobe University, 109-122.

Miller, A.J., 2002: *Subset Selection in Regression*. Chapman&Hall/CRC, Boca Raton.

Moreno-Garcia, M.C., 1994: Intensity and form of the urban heat island in Barcelona. *Int. J. Climatol. 14*, 705-710.

Morris, C.J.G., Simmonds, I., and *Plummer, N.*, 2001: Quantification of the influences of wind and cloud on the nocturnal urban heat island of a large city. *J. Appl. Meteorol. 40*, 169-182.

Myrup, L.O., McGinn, C.E., and *Flocchini, R.G.*, 1993: An analysis of microclimatic variation in a suburban environment. *Atmos. Environ. 27B*, 129-156.

Nkemdirim, L.C., 1978: Variability of temperature fields in Calgary, Alberta. *Atmos. Environ. 12*, 809-822.

Nkemdirim, L.C., 1980: A test of lapse rate/wind speed model for estimating heat island magnitude in an urban airshed. *J. Appl. Meteorol. 19*, 748-756.

Oke, T.R., 1973: City size and the urban heat island. *Atmos. Environ. 7*, 769-779.

Oke, T.R., 1976: The distinction between canopy and boundary layer urban heat islands. *Atmosphere 14*, 268-277.

Oke, T.R., 1981: Canyon geometry and the nocturnal urban heat island: comparison of scale model and field observations. *J. Climatol. 1*, 237-254.

Oke, T.R., 1987: *Boundary Layer Climates*. Routledge. London and New York, 405 pp.

Oke, T.R., 1988: Street design and urban canopy layer climate. *Energ. Buildings 11*, 103-113.

Oke, T.R. and *Fuggle, R.F.*, 1972: Comparison of urban/rural counter and net radiation at night. *Bound.-Lay. Meteorol. 2*, 290-308.

Oke, T.R. and *Maxwell, G.B.*, 1975: Urban heat island dinamics in Montreal and Vancouver. *Atmos. Environ. 9*, 191-200.

Outcalt, S.I., 1972: A synthetic analysis of seasonal influences in the effects of land use on the urban thermal regime. *Arch. Meteor. Geophy. B 20*, 253-260.

Park, H.-S., 1986: Features of the heat island in Seoul and its surrounding cities. *Atmos. Environ. 20*, 1859-1866.

Park, H.-S., 1987: Variations in the urban heat island intensity affected by geographical environments. *Environmental Research Center Papers 11*. The University of Tsukuba, Ibaraki, Japan, 79 pp.

Ruffieux, D., 1995: Winter surface energy budget in Denver, Colorado. *Atmos. Environ. 29*, 1579-1587.

Sundborg, A., 1950: Local climatological studies of the temperature conditions in an urban area. *Tellus 2*, 222-232.

Tapper, P.D., Tyson, P.D., Owens, I.F., and *Hastie, W.J.*, 1981: Modeling the winter urban heat island over Christchurch. *J. Appl. Meteorol. 20*, 365-367.

Unger, J., 1996: Heat island intensity with different meteorological conditions in a medium-sized town: Szeged, Hungary. *Theor. Appl. Climatol. 54*, 147-151.

Unger, J., 1999: Urban-rural air humidity diferences in Szeged, Hungary. *Int. J. Climatol. 19*, 1509-1515.

Unger, J., Bottyán, Z., Sümeghy, Z., and *Gulyás, A.*, 2000: Urban heat island development affected by urban surface factors. *Időjárás 104*, 253-268.

Unger, J., Sümeghy, Z., and *Zoboki, J.*, 2001: Temperature cross-section features in an urban area. *Atmos. Res. 58*, 117-127.

Voogt, J.A. and *Oke, T.R.*, 1991: Validation of an urban canyon radiation model for nocturnal long-wave radiative fluxes. *Bound.-Lay. Meteorol. 54*, 347-361.

Voogt, J.A. and *Oke, T.R.*, 1997: Complete urban surface temperatures. *J. Appl. Meteorol. 36*, 1117-1132.

Voogt, J.A. and *Grimmond, C.S.B.*, 2000: Modeling surface sensible heat flux using surface radiative temperatures in a simple urban area. *J. Appl. Meteorol. 39*, 1679–1699.

Yagüe, C., Zurita, E., and *Martinez, A.*, 1991: Statistical analysis of the Madrid urban heat island. *Atmos. Environ. 25B*, 327-332.

Yamashita, S., 1996: Detailed structure of heat island phenomena from moving observations from electric tram-cars in metropolitan Tokyo. *Atmos. Environ. 30*, 429-435.

Yamashita, S., Sekine, K., Shoda, M., Yamashita, K., and *Hara, Y.*, 1986: On the relationships between heat island and sky view factor in the cities of Tama River Basin, Japan. *Atmos. Environ. 20*, 681-686.